Miscoding Potential of the N^2-Ethyl-2′-deoxyguanosine DNA Adduct by the Exonuclease-Free Klenow Fragment of *Escherichia coli* DNA Polymerase I†

Isamu Terashima,‡ Tomonari Matsuda,§ Tzan-Wei Fang,‡ Naomi Suzuki,‡ Jun Kobayashi,|| Kohfuku Kohda,*,|| and Shinya Shibutani*,‡

Laboratory of Chemical Biology, Department of Pharmacological Sciences, State University of New York at Stony Brook, Stony Brook, New York 11794-8651, Research Center for Environmental Quality Control, Kyoto University, 1-2 Yumihama, Otsu, Shiga 520, Japan, and Faculty of Pharmaceutical Sciences, Nagoya City University, Tanabe-dori, Mizuho-ku, Nagoya 467, Japan

Received November 28, 2000; Revised Manuscript Received January 30, 2001

ABSTRACT: Acetaldehyde, a major metabolite of ethanol, reacts with dG residues in DNA, resulting in the formation of the N^2-ethyl-2′-deoxyguanosine (N^2-Et-dG) adduct. This adduct has been detected in lymphocyte DNA of alcohol abusers. To explore the miscoding property of the N^2-Et-dG DNA adduct, phosphoramidite chemical synthesis was used to prepare site-specifically modified oligodeoxynucleotides containing a single N^2-Et-dG. These N^2-Et-dG-modified oligodeoxynucleotides were used as templates for primer extension reactions catalyzed by the 3′ → 5′ exonuclease-free (exo$^-$) Klenow fragment of *Escherichia coli* DNA polymerase I. The primer extension was retarded one base prior to the N^2-Et-dG lesion and opposite the lesion; however, when the enzyme was incubated for a longer time or with increased amounts of this enzyme, full extension occurred. Quantitative analysis of the fully extended products showed the preferential incorporation of dGMP and dCMP opposite the N^2-Et-dG lesion, accompanied by a small amounts of dAMP and dTMP incorporation and one- and two-base deletions. Steady-state kinetic studies were also performed to determine the frequency of nucleotide insertion opposite the N^2-Et-dG lesion and chain extension from the 3′ terminus from the dN·N^2-Et-dG (N is C, A, G, or T) pairs. These results indicate that the N^2-Et-dG DNA adduct may generate G → C transversions in living cells. Such a mutational spectrum has not been detected with other methylated dG adducts, including 8-methyl-2′-deoxyguanosine, O^6-methyl-2′-deoxyguanosine, and N^2-methyl-2′-deoxyguanosine. In addition, N^2-ethyl-2′-deoxyguanosine triphosphate (N^2-Et-dGTP) was efficiently incorporated opposite a template dC during DNA synthesis catalyzed by the exo$^-$ Klenow fragment. The utilization of N^2-Et-dGTP was also determined by steady-state kinetic studies. N^2-Et-dG DNA adducts are also formed by the incorporation of N^2-Et-dGTP into DNA and may cause mutations, leading to the development of alcohol- and acetaldehyde-induced human cancers.

Acetaldehyde is produced in the body due to alcoholic beverage consumption via the metabolic oxidation of ethanol. This chemical agent is present in many foods, automotive exhaust gases (*1*), and cigarette smoke (*2*). Acetaldehyde is also produced from endogenous sources such as threonine, *β*-alanine, and deoxyribose phosphate during normal intermediary metabolism (*3*, *4*). Treatment with acetaldehyde promotes adenocarcinomas, squamous cell carcinomas, and laryngeal carcinomas in rodents (*1*). Esophageal squamous cell carcinoma is associated with alcohol and tobacco consumption (*5*). Alcohol dehydrogenase gene 2 and aldehyde dehydrogenase gene 2 genetic polymorphism is also related to development of human esophageal and liver cancer (*6*). Acetaldehyde induces sister chromatid exchanges in bone marrow cells of rodents (*7*, *8*) and in cultured human lymphocytes (*9*), chromosomal aberrations in rat embryos (*10*), and mutations in cultured human skin fibroblasts (*11*). This chemical also induces intrastrand DNA cross-links between adjacent guanine bases and tandem GG → TT base substitutions in shuttle vector plasmids propagated in human fibroblast cells (*12*). Acetaldehyde is therefore considered to be a possible carcinogen in humans by the International Agency for Research on Cancer (*13*).

Acetaldehyde induces the formation of a Schiff base at exocyclic amino groups of 2′-deoxyguanosine, which can be reduced by glutathione and ascorbic acid in cells, to form the stable N^2-ethyl-2′-deoxyguanosine (N^2-Et-dG)[1] (*14*)

† A preliminary report of this study was presented at the 91st Annual Meeting of the American Association for Cancer Research, April 2000, in San Francisco, CA. Research supported in part by Grants-in-Aid 08555137 and 09750636 from the Ministry of Education, Science, Sports and Culture of Japan (to T.M.) and Grants ES09418 and ES04068 from the National Institute of Environmental Health Sciences (to S.S.).

* To whom correspondence should be addressed. K.K.: phone, +81-52-836-3798; fax, +81-52-834-9309; e-mail, kohda@phar.nagoya-cu.ac.jp. S.S.: phone, (631) 444-8018; fax, (631) 444-3218; e-mail, shinya@pharm.sunysb.edu.

‡ State University of New York at Stony Brook.

§ Kyoto University.

|| Nagoya City University.

[1] Abbreviations: N^2-Et-dG, N^2-ethyl-2′-deoxyguanosine; dGTP, 2′-deoxyguanosine triphosphate; N^2-Et-dGTP, N^2-ethyl-2′-deoxyguanosine triphosphate; exo$^-$ KF, 3′ → 5′ exonuclease-free Klenow fragment of *Escherichia coli* DNA polymerase I; PAGE, polyacrylamide gel electrophoresis; HPLC, high-performance liquid chromatography.

10.1021/bi002719p CCC: $20.00
Published on Web 03/08/2001

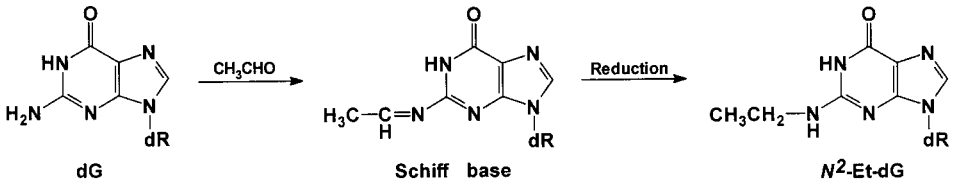

FIGURE 1: Formation of N^2-Et-dG through a Schiff base.

Scheme 1

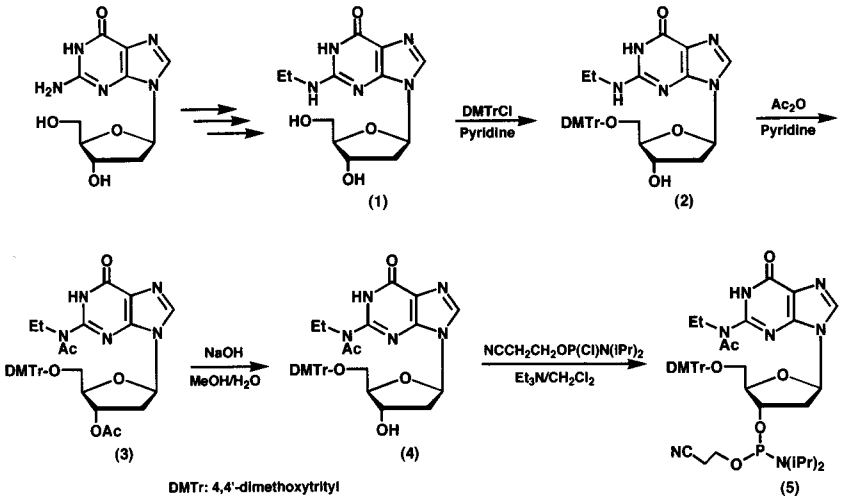

(Figure 1). N^2-Et-dG-DNA adducts were detected in the liver of mice treated with ethanol (*14*) and in the granulocytes and lymphocytes of alcoholic patients (*15*). N^2-Et-dG was also detected in human urine samples obtained from healthy non-alcohol drinkers and nonsmokers (*16*). These indicate that humans are exposed to acetaldehyde, and it may be involved in the development of cancers.

N^2-Et-dG excreted in urine may result from decomposition of N^2-Et-modified nucleotides such as N^2-ethyl-2′-deoxyguanosine triphosphate (N^2-Et-dGTP) and repair of N^2-Et-dG adducts in cellular DNA. We have recently determined the utilization of N^2-Et-dGTP during DNA synthesis catalyzed by mammalian DNA polymerases (*16*). N^2-Et-dGTP was efficiently incorporated into DNA; the level of utilization of N^2-Et-dGTP was much higher than that of 7,8-dihydro-8-oxo-2′-deoxyguanosine triphosphate (8-oxo-dGTP), a typical oxidatively damaged nucleotide. Thus, modification of deoxynucleoside 5′-triphosphate may play an important role in mutagenesis and carcinogenesis.

To explore the miscoding potential of the N^2-Et-dG adduct, a phosphoramidite chemical synthesis was established to prepare site-specifically modified oligodeoxynucleotides containing a single N^2-Et-dG adduct. Using N^2-Et-dG-modified oligodeoxynucleotide templates and the 3′ → 5′ exonuclease-free Klenow fragment (exo$^-$ KF) of *Escherichia coli* DNA polymerase I, the miscoding specificity and frequency of deoxynucleotides opposite the N^2-Et-dG adduct were investigated by an in vitro experimental system that can quantify base substitutions and deletions (*17*, *18*) and steady-state kinetic analysis. Utilization of N^2-Et-dGTP during DNA synthesis was also assessed. We found that N^2-Et-dGTP was efficiently incorporated into DNA and that the resultant N^2-Et-dG adduct has high miscoding potential, generating a unique miscoding spectrum, G → C transversions.

MATERIALS AND METHODS

Synthesis of N^2-Et-dG Derivatives. (1) General. ^{1}H NMR spectra were recorded on a GSX 400 spectrometer (JEOL, Tokyo, Japan), and chemical shifts were reported in parts per million (ppm) using tetramethylsilane as the internal standard. Mass spectra were recorded on a JMS-DX300 spectrometer (JEOL) or Voyager-Elite Biospectrometry Workstation (PerSeptive Biosystems). HPLC analyses were carried out using a LC-10AD apparatus equipped with a photodiode array SPD-M10A UV detector (Shimadzu, Kyoto, Japan). A LiChrospher 100 RP-18(e) column (250 mm × 4 mm) (Merck) was used, and the elution conditions that were employed were described in the text. Silica gel 60 PF254 (Merck) was used for preparative thin-layer chromatography (PLC) and developed with a solvent system (9:1 $CHCl_3$/MeOH mixture).

(2) 5′-O-(4,4′-Dimethoxytrityl)-N^2-ethyl-2′-deoxyguanosine (2). As shown in Scheme 1, N^2-Et-dG (**1**) was prepared from 2′-deoxyguanosine following the procedure reported previously (*19*). N^2-Et-dG (**1**, 300 mg, 1.01 mmol), 4-(dimethylamino)pyridine (6.1 mg, 0.05 equiv), and triethylamine (212 μL, 1.5 equiv) were dissolved in dry pyridine (15 mL). 4,4′-Dimethoxytrityl chloride (513 mg, 1.5 equiv) was then added, and the mixture was stirred at room temperature for 2 h. Water (15 mL) was poured into the reaction mixture, and the product was extracted with diethyl ether (3 × 20 mL). The organic layer was dried with anhydrous $MgSO_4$. After removal of the solvent, 5′-*O*-(4,4′-dimethoxytrityl)-N^2-ethyl-2′-deoxyguanosine (**2**) was isolated by PLC as a white powder in 68% yield (411 mg). The R_f values of **1** and **2** were 0.05 and 0.22, respectively: ^{1}H NMR (DMSO-d_6) δ 1.05 (t, 3H, J = 7.2 Hz, CH_2CH_3), 2.25 (m, 1H, 2′-Ha), 2.66 (m, 1H, 2′-Hb), 3.30 (m, 4H, CH_2CH_3 and 5′-H), 3.72 (s, 6H, OCH_3), 3.92 (m, 1H, 4′-H), 4.40 (m, 1H, 3′-H), 5.31 (br d, 1H, J = 4.6 Hz, 3′-OH), 6.18 (t, 1H, J = 6.2 Hz,

1′-H), 6.51 (br s, 1H, 2-NH), 6.80−7.69 (m, 13H, phenyl H of trityl), 7.76 (s, 1H, 8-H), 10.57 (br s, 1H, 1-NH); FAB-MS *m*/*z* 598 [(M + H)$^+$].

(3) N^2,3′-O-Diacetyl-5′-O-(4,4′-dimethoxytrityl)-N^2-ethyl-2′-deoxyguanosine (3). Compound **2** (200 mg, 0.33 mmol) was dissolved in pyridine (6 mL). Acetic anhydride (197 mL, 8 equiv) and triethylamine (272 mL, 9 equiv) were added, and the mixture was kept standing at 40 °C for 3 h. After removal of the solvent, N^2,3′-*O*-diacetyl-5′-*O*-(4,4′-dimethoxytrityl)-N^2-ethyl-2′-deoxyguanosine (**3**) was isolated by PLC as a viscous residue in 83% yield (190 mg). The R_f value of **3** was 0.51: ^{1}H NMR (DMSO-d_6) δ 1.02 (t, 3H, J = 7.0 Hz, CH_2CH_3), 2.05 and 2.08 (each s, each 3H, each $COCH_3$), 2.91−3.25 (m, 2H, 5′-H), 3.68 (m, 2H, CH_2CH_3), 3.71 and 3.72 (each s, each 3H, each OCH_3), 4.15 (m, 1H, 4′-H), 5.35 (m, 1H, 3′-H), 6.32 (t, 1H, J = 6.8 Hz, 1′-H), 6.76∼7.31 (m, 13H, phenyl H of trityl), 8.20 (s, 1H, 8-H).

(4) N^2-Acetyl-5′-O-(4,4′-dimethoxytrityl)-N^2-ethyl-2′-deoxyguanosine (4). Compound **3** (150 mg, 0.22 mmol) was dissolved in $CHCl_3$ (2 mL). MeOH (10 mL) and an aqueous 1 N NaOH solution (10 mL) were added, and the mixture was kept stirring at room temperature for 30 min. The product was extracted with $CHCl_3$ (3 × 5 mL). The organic layer was dried with anhydrous $MgSO_4$. After removal of the solvent, N^2-acetyl-5′-*O*-(4,4′-dimethoxytrityl)-N^2-ethyl-2′-deoxyguanosine (**4**) was isolated by PLC as a viscous residue in 77% yield (108 mg). The R_f value of **4** was 0.39: ^{1}H NMR (DMSO-d_6) δ 1.02 (t, 3H, J = 7.1 Hz, CH_2CH_3), 2.06 (s, 3H, $COCH_3$), 2.35 (m, 1H, 2′-Ha), 2.72 (m, 1H, 2′-Hb), 3.13 (m, 2H, 5′-H), 3.68 (q, 2H, J = 7.1 Hz, CH_2CH_3), 3.71 and 3.72 (each s, each 3H, each OCH_3), 3.97 (m, 1H, 4′-H), 4.38 (m, 1H, 3′-H), 5.35 (br s, J = 4.7 Hz, 1H, 3′-OH), 6.30 (t, 1H, J = 6.3 Hz, 1′-H), 6.30 (br s, 1H, 2-NH), 6.76∼7.29 (m, 13H, phenyl H of trityl), 8.20 (s, 1H, 8-H), 12.70 (br s, 1H, 1-NH); FAB-MS *m*/*z* 640 [(M + H)$^+$]. By heating compound **4** in 25% NH_4OH at 55 °C for 15 h, the conditions commonly used for deblocking, we could deblock the acetyl group of **4** and form compound **2**.

(5) 3′-O-[(2-Cyanoethoxy)(diisopropylamino)phosphino]-N^2-acetyl-5′-O-(4,4′-dimethoxytrityl)-N^2-ethyl-2′-deoxyguanosine (5). Compound **4** (108 mg, 0.17 mmol) was dried over P_2O_5 and coevaporated with dry CH_2Cl_2 and benzene. CH_2Cl_2 (2 mL), triethylamine (59 μL, 2.5 equiv), and 2-cyanoethyl *N*,*N*-diisopropylchlorophosphoramidite (57 μL, 1.5 equiv) were added, and the mixture was stirred at room temperature for 30 min. The solvent was removed by evaporation, and a THF/benzene mixture (1:4, 5 mL) was added. After the precipitate had been removed by filtration, the solvent was removed by evaporation. Coevaporation of the residue with dry benzene (2 × 5 mL) gave 3′-*O*-[(2-cyanoethoxy)(diisopropylamino)phosphino]-N^2-acetyl-5′-*O*-(4,4′-dimethoxytrityl)-N^2-ethyl-2′-deoxyguanosine (**5**). The yield of **5** was more than 80% judging from the TLC spots of the reaction mixture. The R_f value of **5** was 0.45 (silica gel, 9:1 $CHCl_3$/MeOH mixture). Without further purification, the product was dried over P_2O_5 and used for subsequent oligodeoxynucleotide synthesis.

Preparation of Oligodeoxynucleotides Containing a Single N^2-Et-dG. Oligodeoxynucleotides containing an N^2-Et-dG (5′CCTTCXCTTCTTTCCTCTCCCTTT and 5′CATGCTGTTGAATTCCTTCXCTTCTTTCCTCTCCCTTT, where X is N^2-Et-dG) were prepared by the phosphoramidite method on a solid-phase DNA synthesizer (Applied Biosystems model 392) at the 1 mmol scale under autocleavage trityl-on mode. Deprotection of the oligodeoxynucleotide was carried out with 25% NH_4OH at 55 °C for 15 h. The oligodeoxynucleotide was purified by HPLC [65 mM phosphate buffer (pH 7.0) and MeOH] and further on an OPC column (Applied Biosystems), and then was detritylated. Unmodified DNA templates (5′CCTTCGCTTCTTTCCTCTCCCTTT and 5′CATGCTGTTGAATTCCTTCGCTTCTTTCCTCTCCCTTT), primers, and standard markers listed in Figure 2 were prepared by the phosphoramidite method using an automated DNA synthesizer (*20*). The template sequences were not selected from a particular gene and were chosen for quantitative miscoding analysis using two-phase polyacrylamide gel electrophoresis (PAGE) (*17*, *18*). The unmodified and N^2-Et-dG-modified oligodeoxynucleotides were further purified on a Waters reverse-phase μBondapak C_{18} column (0.39 cm × 30 cm) using an isocratic condition of 0.05 M triethylammonium acetate (pH 7.0) containing 5% acetonitrile for 5 min and subsequently a linear gradient of 0.05 mM triethylammonium acetate (pH 7.0) containing 5 → 20% acetonitrile with an elution time of 55 min at a flow rate of 1.0 mL/min. A Waters 990 HPLC instrument, equipped with a photodiode array detector, was used for the separation and purification of the oligodeoxynucleotides.

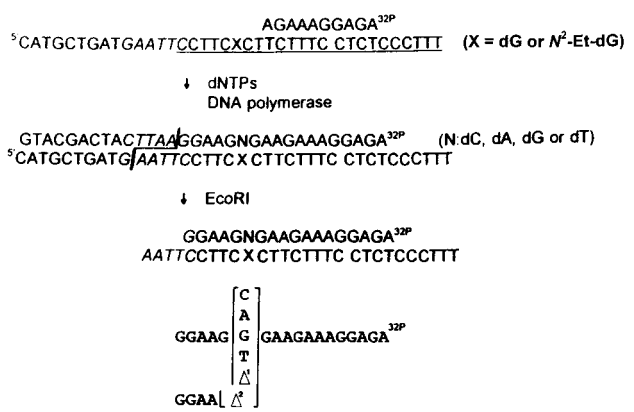

FIGURE 2: Diagram of a method used to determine miscoding specificities.

Enzymatic Digestion of N^2-Et-dG-Modified Oligodeoxynucleotides. To prove that N^2-Et-dG was incorporated into the oligodeoxynucleotides, a portion of the N^2-Et-dG-modified oligodeoxynucleotide was hydrolyzed to deoxynucleosides using spleen phosphodiesterase and alkaline phosphatase, as described previously (*21*). Briefly, the N^2-Et-dG-modified oligodeoxynucleotide (3 μg) was digested at 37 °C for 2 h with spleen phosphodiesterase (0.1 unit) and alkaline phosphatase (3 units) in 100 μL of a 30 mM sodium acetate buffer (pH 5.3) containing 5 μL of 20 mM zinc sulfate. Nucleosides were extracted twice with MeOH and analyzed by HPLC. Elution was performed with a linear gradient of MeOH in 65 mM phosphate buffer (pH 6.8) at a flow rate of 0.8 mL/min (from 0 to 15% MeOH over the course of 20 min and then from 15 to 100% MeOH over the course of 80 min).

Mass Spectrometry of Oligodeoxynuculeotides. Ten microliters of 0.5 M 2,4,6-trihydroxyacetophenone in ethanol and 5 μL of 0.1 M diammonium hydrogen citrate in H_2O were mixed. One microliter of an oligodeoxyribonucleotide solution (5 OD/mL) in H_2O was then added, and the mixture

was vortexed. After 1.0 μL of this solution had been loaded onto the sample plate and the solvent removed, the molecular mass of oligodeoxynucleotides was measured by MALDI-TOF/MS. The process yielded the exact molecular mass of the oligomer containing N^2-Et-dG.

Synthesis of N^2-Et-dGTP. N^2-Et-dGTP was prepared as described previously (*16*). Briefly, dGTP (3 mg) was reacted overnight with 0.1 mL of acetaldehyde in 1 mL of 0.2 mM sodium acetate buffer (pH 4.5) and reduced by $NaBaH_4$. N^2-Et-dGTP was purified on a reverse-phase μBondapak C_{18} column (0.39 cm × 30 cm, Waters), using a linear gradient of 0.05 M triethylammonium acetate (pH 7.0) containing 0 → 50% acetonitrile, with an elution time of 40 min and a flow rate of 1.0 mL/min.

Experiments for the Primer Extension Reaction. (1) General. [γ-^{32}P]ATP (specific activity > 6000 Ci/mmol) was obtained from Amersham Corp. dNTPs were from Pharmacia. T4 polynucreotide kinase was from Stratagene. The cloned exo$^-$ Klenow fragment of DNA polymerase I (21 200 units/mg) was purchased from United States Biochemical Corp.

(2) Primer Extension Reaction. Using a modified or unmodified 38-mer oligodeoxynucleotide (5′CATGCTGTTGAATTCCTTCXCTTCTTTCCTCTCCCTTT, where X is dG or N^2-Et-dG, 0.75 pmol) primed with a ^{32}P-labeled 10-mer (5′AGAGGAAAGA, 0.5 pmol), primer extension reactions catalyzed by the exo$^-$ KF were conducted at 25 °C in a buffer (10 μL) containing four dNTPs (100 μM each). The reaction buffer for the exo$^-$ KF contained 50 mM Tris-HCl (pH 8.0), 8 mM $MgCl_2$, and 5 mM 2-mercaptoethanol. The reaction was stopped by addition of formamide dye. The samples were subjected to 20% denaturing PAGE. The radioactivities of the extended products were measured with a β-phosphorimager (Molecular Dynamics).

Quantitation of the Miscoding Specificity. The fully extended reaction products (approximately 32 bases long) were extracted from the gel. The recovered oligodeoxynucleotides were annealed with an unmodifed 38-mer and cleaved with *Eco*RI. To quantify all base substitutions and deletions, the samples were subjected to two-phase PAGE (15 cm × 72 cm × 0.04 cm) (*17*, *18*) (Figure 2).

Steady-State Kinetic Studies. Kinetic parameters associated with nucleotide insertion opposite the N^2-Et-dG lesion and chain extension from the 3′ primer terminus were determined at 25 °C, using the reaction conditions that included varying amounts of a single dNTP. To measure the nucleotide insertion kinetics, reaction mixtures containing 0.001−0.5 unit of the exo$^-$ KF and varying amounts of a single dNTP were incubated at 25 °C for 2 min in 10 μL of Tris-HCl buffer (pH 8.0) using a 24-mer template (0.75 pmol, 5′CCTTCXCTTCTTTCCTCTCCCTTT, where X is dG or N^2-Et-dG) primed with a ^{32}P-labeled 12-mer (0.5 pmol, 5′AGAGGAAAGAAG). Reaction mixtures containing 1.0 pmol of 24-mer template primed with 0.5 pmol of a ^{32}P-labeled 13-mer (5′AGAGGAAAGAAGN, where N is C, A, G, or T) and varying amounts of dGTP were used to assess chain extension. The reaction samples were subjected to 20% denaturating PAGE (35 cm × 42 cm × 0.04 cm). The Michaelis constants (K_m) and maximum rates of reaction (V_{max}) were obtained from Hanes−Woolf plots.

Kinetics of Insertion of N^2-Et-dGTP into DNA Templates.

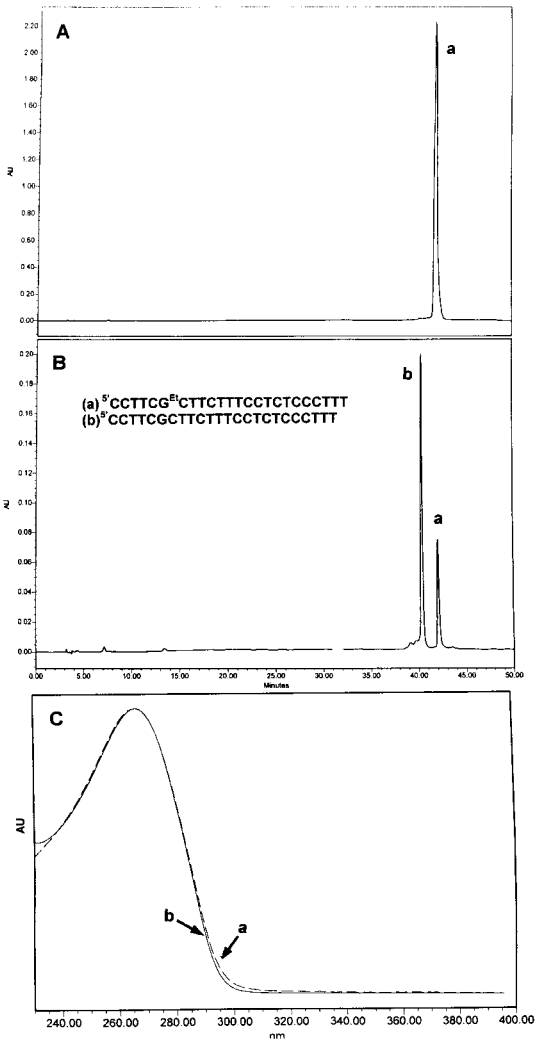

FIGURE 3: HPLC separation of an oligodeoxynucleotide containing a single N^2-Et-dG. (A) The N^2-Et-dG-modified oligodeoxynucleotide was prepared by phosphoramidite chemical synthesis as described in Materials and Methods. The N^2-Et-dG-modified 24-mer was isolated on a reverse-phase μBondapak C_{18} column (0.39 cm × 30 cm), using an isocratic condition of 0.05 M triethylammonium acetate (pH 7.0) containing 5% acetonitrile for 5 min and subsequently a linear gradient of 0.05 mM triethylammonium acetate (pH 7.0) containing 5 → 20% acetonitrile with an elution time of 55 min at a flow rate of 1.0 mL/min. (B) HPLC isolation of the N^2-Et-dG-modified 24-mer (a) and the corresponding unmodified 24-mer (b). (C) UV spectra of the N^2-Et-dG-modified 24-mer (a) and the unmodified 24-mer (b).

A 24-mer template (0.75 pmol, 5′CCTTCNCTTCTTTCCTCTCCCTTT, where N is C, A, G, or T) primed with a ^{32}P-labeled 12-mer (0.5 pmol, 5′AGAGGAAAGAAG) was used for determination of the level of dGTP or N^2-Et-dGTP incorporation opposite the dC, dA, dG, or dT embedded in the template (*16*). Steady-state kinetic parameters were established for N^2-Et-dGTP or dGTP insertion opposite dN in templates using the exo$^-$ KF. Reaction mixtures containing 0.001−0.5 unit of the exo$^-$ KF and varying amounts of N^2-Et-dGTP or dGTP were incubated at 25 °C for 2 min in 10 μL of the buffer containing a 24-mer template (1.0 pmol) primed with a ^{32}P-labeled 12-mer (0.5 pmol). Reaction samples were subjected to electrophoresis on 20% polyacrylamide gels (35 cm × 42 cm × 0.04 cm) in the presence of 7 M urea. K_m and V_{max} were obtained from Hanes−Woolf plots. Frequencies of insertion (F_{ins}) were determined relative

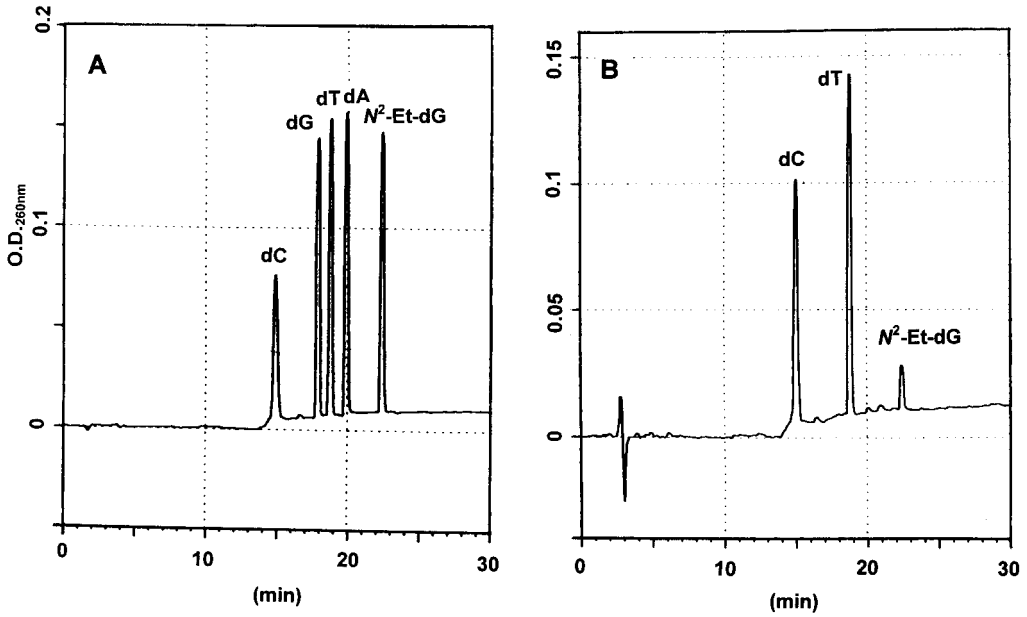

FIGURE 4: Enzymatic digestion of the N^2-Et-dG-modified 24-mer oligodeoxynucleotide. (A) A standard mixture of deoxynucleosides and N^2-Et-dG was passed through a Supelcosil LC-18S column. The column was eluted with a linear gradient of 65 mM phosphate buffer (pH 6.8) containing 0 → 15% methanol over the course of 20 min and, subsequently, with 15 → 100% methanol over the course of 80 min at a flow rate of 0.8 mL/min. (B) Three micrograms of N^2-Et-dG-modified 24-mer was hydrolyzed to deoxynucleosides using spleen phosphodiesterase and alkaline phosphatase as described in Materials and Methods. The methanol extract of the digests was evaporated to dryness and analyzed by HPLC.

to the dC·dG base pair according to the equation $F = (V_{max}/K_m)_{[wrong\ pair]}/(V_{max}/K_m)_{[correct\ pair=dC\cdot dG]}$ (*22*, *23*).

RESULTS

Preparation of N^2-Et-dG-Modified Oligodeoxynucleotides by Chemical Synthesis. N^2-Et-dG was prepared using the established procedure (*19*). The 5′-hydroxyl group of N^2-Et-dG was protected by the dimethoxytrityl group. The 2-ethylamino group was then protected by the acetyl group as shown in Scheme 1. The phosphoramidite derivative of compound **5** was prepared by the established protocol (*24*) and used for the solid-phase synthesis of oligodeoxynucleotides containing a single N^2-Et-dG as described in Materials and Methods. The acetyl group of the 2-(*N*-acetyl-*N*-ethylamino) group was removed under alkaline conditions that were used for deblocking the protective groups at the final stage of the oligonucleotides synthesis.

After purification by HPLC, the resulting N^2-Et-dG-modified 24-mer (5′CCTTCXCTTCTTTCCTCTCCCTTT, where X is N^2-Et-dG) was isolated at 42.1 min by HPLC (Figure 3A). This modified 24-mer can be resolved from the unmodified 24-mer (t_R = 40.4 min) as shown in Figure 3B. The UV spectrum of the N^2-Et-dG-modified 24-mer was similar to that of the unmodified 24-mer (Figure 3C).

To confirm the incorporation of Et-N^2-dG into the oligodeoxynucleotide, a portion of the N^2-Et-dG-modified 24-mer was digested with spleen phosphodiesterase and alkaline phosphatase. The resultant deoxynucleotides were analyzed by HPLC. The retention times of authentic dC, dA, dT, dG, and N^2-Et-dG were 14.9, 17.8, 18.7, 20.0, and 22.5 min, respectively (Figure 4A). When the digested sample was subjected to HPLC, only dC, dT, and N^2-Et-dG were detected (Figure 4B); the molecular dC:dT:N^2-Et-dG ratio was consistent with the theoretical value (11:12:1) of the deoxynucleoside composition of the N^2-Et-dG-modified 24-mer.

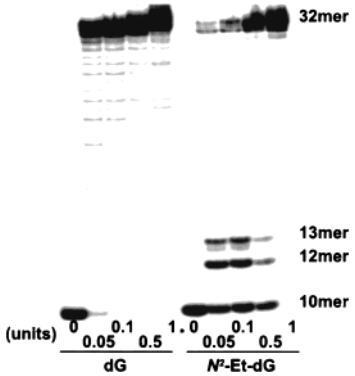

FIGURE 5: Primer extension reactions catalyzed by the exo⁻ Klenow fragment. Using unmodified or N^2-Et-dG-modified 38-mer templates (5′CATGCTGTTGAATTCCTTCXCTTCTTTCCTCTCCCTTT, where X is dG or N^2-Et-dG) primed with a ^{32}P-labeled 10-mer (5′AGAGGAAAGA), primer extension reactions were conducted at 25 °C for 1 h in a buffer containing four dNTPs (100 μM each) and variable amounts of the exo⁻ KF as described in Materials and Methods. One-third of the reaction mixture was subjected to the denaturing 20% polyacrylamide gel electrophoresis (35 cm × 42 cm × 0.04 cm). The radioactivities of extended products were measured by a β-phosphorimager.

Primer Extension Reaction Catalyzed by the Exo⁻ Klenow Fragment. Using unmodified and N^2-Et-dG-modified 38-mer templates, primer extension reactions were conducted in the presence of four dNTPs using variable amounts of the exo⁻ KF (Figure 5). The primer extension readily occurred on the unmodified template to form the fully extended products. In contrast, when an N^2-Et-dG-modified template was used, the extension reaction was retarded one base prior to the N^2-Et-dG lesion and opposite the lesion. Two bands remained at position 13. The upper and lower bands represented the incorporation of dGMP and dCMP, respectively, opposite the lesion, as demonstrated previously (*25*). Full extension

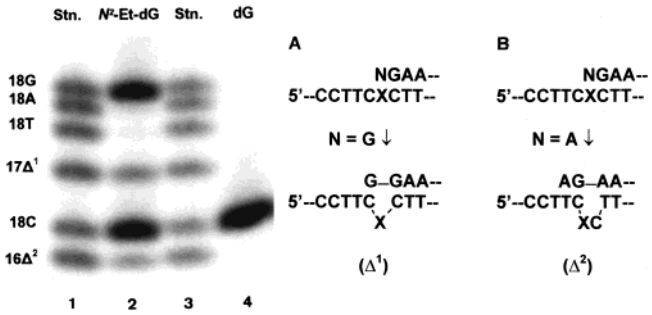

FIGURE 6: Quantification of miscoding specificities induced by the N^2-Et-dG adduct. As shown in Figure 5, the fully extended reaction products produced on the unmodified or N^2-Et-dG-modified template using 1.0 unit of the exo$^-$ KF were extracted from PAGE. The recovered oligodeoxynucleotides were annealed with an unmodified 38-mer and cleaved with the *Eco*RI restriction enzyme as described in Materials and Methods. The reaction samples were subjected to a two-phase 20% polyacrylamide gel electrophoresis (15 cm × 72 cm × 0.04 cm). The mobilities of the reaction products were compared with those of 18-mer standards (Figure 2) containing dC, dA, dG, or dT opposite the lesion and one-base (Δ^1) or two-base (Δ^2) deletions. Proposed mechanisms of one- and two-base deletions are described in panels A and B, respectively.

could be obtained by increasing the amount of the exo$^-$ KF (Figure 5).

Miscoding Property of the N^2-Et-dG Adduct. After the fully extended products were recovered from the gel and digested with *Eco*RI, the products were subjected to two-phase PAGE to quantify all base substitutions and deletions formed opposite the N^2-Et-dG lesion during DNA synthesis (Figure 2). The standard mixture of six ^{32}P-labeled oligodeoxynucleotides containing dC, dA, dG, or dT opposite the lesion and one- or two-base deletions is resolved by this method (Figure 6, lanes 1 and 3). When the unmodified template was used, only the correct base, dCMP, was inserted opposite dG (lane 4). N^2-Et-dG directed the incorporation of both dGMP (40%) and dCMP (39%), along with a small amount of dAMP (2.2%) and dTMP (1.9%). One-base deletion (9.7%) and two-base deletion (7.1%) were also observed (lane 2).

Kinetic Studies on the N^2-Et-dG-Modified DNA Template. Using steady-state kinetic studies, the frequency of dNTP incorporation (F_{ins}) opposite the N^2-Et-dG lesion was measured. As shown in Table 1 and Figure 7, both the K_m and V_{max} of dGTP insertion opposite the N^2-Et-dG lesion were 2.1 times lower than those for dCTP. Therefore, dGTP was incorporated as efficiently as dCTP, the correct base. The frequencies of dATP and dTTP insertion were 12 and 39 times lower than that of dCTP insertion, respectively. Chain extension reactions were carried out in the presence of dGTP. The dC·N^2-Et-dG pair was extended more frequently than other pairs (Table 1 and Figure 7). The F_{ext} values of the dT·N^2-Et-dG, dG·N^2-Et-dG, and dA·N^2-Et-dG pairs were 110, 920, and 11 100 times lower, respectively, than that of the dC·N^2-Et-dG pair.

The relative frequency of translesional synthesis ($F_{ins}F_{ext}$) of the dG·N^2-Et-dG pair was therefore 280 times lower than that of the dC·N^2-Et-dG pair, but 100 and 460 times higher than those of the dT·N^2-Et-dG and dA·N^2-Et-dG pairs, respectively.

Insertion of N^2-Et-dGTP into DNA. Using steady-state kinetic studies, the frequency of incorporation of N^2-Et-dGTP or dGTP opposite template dN (dC, dA, dG, or dT) was measured by using the exo$^-$ KF (Table 2). Preferential incorporation of N^2-Et-dGTP opposite template dC, the correct base, was observed. F_{ins} of N^2-Et-dGTP opposite template dC (1.20×10^{-1}) was only 8.3 times lower than that for dGTP. F_{ins} of N^2-Et-dGTP opposite template dG (1.57×10^{-4}) was 760 times lower than that observed opposite template dC and 2.3 and 3.8 times higher than that observed opposite template dA (6.96×10^{-5}) and dT (4.11×10^{-5}), respectively. Thus, N^2-Et-dGTP can be incorporated efficiently into template dC during DNA synthesis.

DISCUSSION

The exo$^-$ KF promoted high levels of incorporation of dGMP (40%), in addition to dCMP (39%), the correct base, opposite the N^2-Et-dG lesion during DNA synthesis. Only small amounts of dAMP and dTMP misincorporation were observed. Therefore, the N^2-Et-dG lesion may primarily generate G → C transversions. This is a unique mutational spectrum when compared to the spectra of the large number of DNA adducts that have been studied.

The resultant G → C transversion observed at the N^2-Et-dG lesion was supported by the kinetic studies. F_{ins} of dGTP opposite the N^2-Et-dG lesion was similar to that for dCTP. However, both F_{ins} values were approximately 1300 times lower than that of dCTP opposite unmodified dG. Therefore, the primer extension reaction may be retarded at a position prior to the N^2-Et-dG lesion. Since the frequencies of chain extension (F_{ext}) from the dC·N^2-Et-dG and dG·N^2-Et-dG pairs were 32 and 29 400 times lower than that for the correct dC·dG pair, the dCMP and dGMP inserted opposite the N^2-Et-dG lesion cannot be readily extended. Therefore, two

Table 1: Kinetic Parameters for Nucleotide Insertion and Chain Extension Reactions Catalyzed by the Exo$^-$ Klenow Fragment[a]

	insertion			extension			
	dNTP ↓GAAGAAAGGAGA^{32p} 5′CCTTCXCTTC TTT CCTCTCCCTTT			dGTP ↓NGAAGAAAGGAGA^{32p} 5′CCTTCXCTTC TTT CCTCTCCCTTT			
N·X	K_m (μM)	V_{max} (% min^{-1})	F_{ins}	K_m (μM)	V_{max} (% min^{-1})	F_{ext}	$F_{ins}F_{ext}$
C·G	0.38 ± 0.12	1850 ± 230	1.0	1.29 ± 0.04	10400 ± 1540	1.0	1.0
C·N^2-Et-dG	72.7 ± 27.3	277 ± 73	7.92×10^{-4}	19.9 ± 3.0	5020 ± 363	3.14×10^{-2}	2.49×10^{-5}
A·N^2-Et-dG	20.0 ± 11.0	6.45 ± 1.70	6.74×10^{-5}	58.6 ± 20.4	1.33 ± 0.05	2.82×10^{-6}	1.90×10^{-10}
G·N^2-Et-dG	35.4 ± 7.1	129 ± 25	7.59×10^{-4}	74.7 ± 36	20.4 ± 2.2	3.40×10^{-5}	8.77×10^{-8}
T·N^2-Et-dG	55.1 ± 23.4	0.81 ± 0.26	3.08×10^{-6}	28.6 ± 9.6	66.8 ± 7.2	2.89×10^{-4}	8.90×10^{-10}

[a] The kinetics of the nucleotide insertion and chain extension reactions were determined as described in Materials and Methods. Frequencies of nucleotide insertion (F_{ins}) and chain extension (F_{ext}) were estimated with the equation $F = (V_{max}/K_m)_{[wrong\ pair]}/(V_{max}/K_m)_{[correct\ pair]}$, where X is dG or N^2-Et-dG. Data are expressed as means ± the standard deviation.

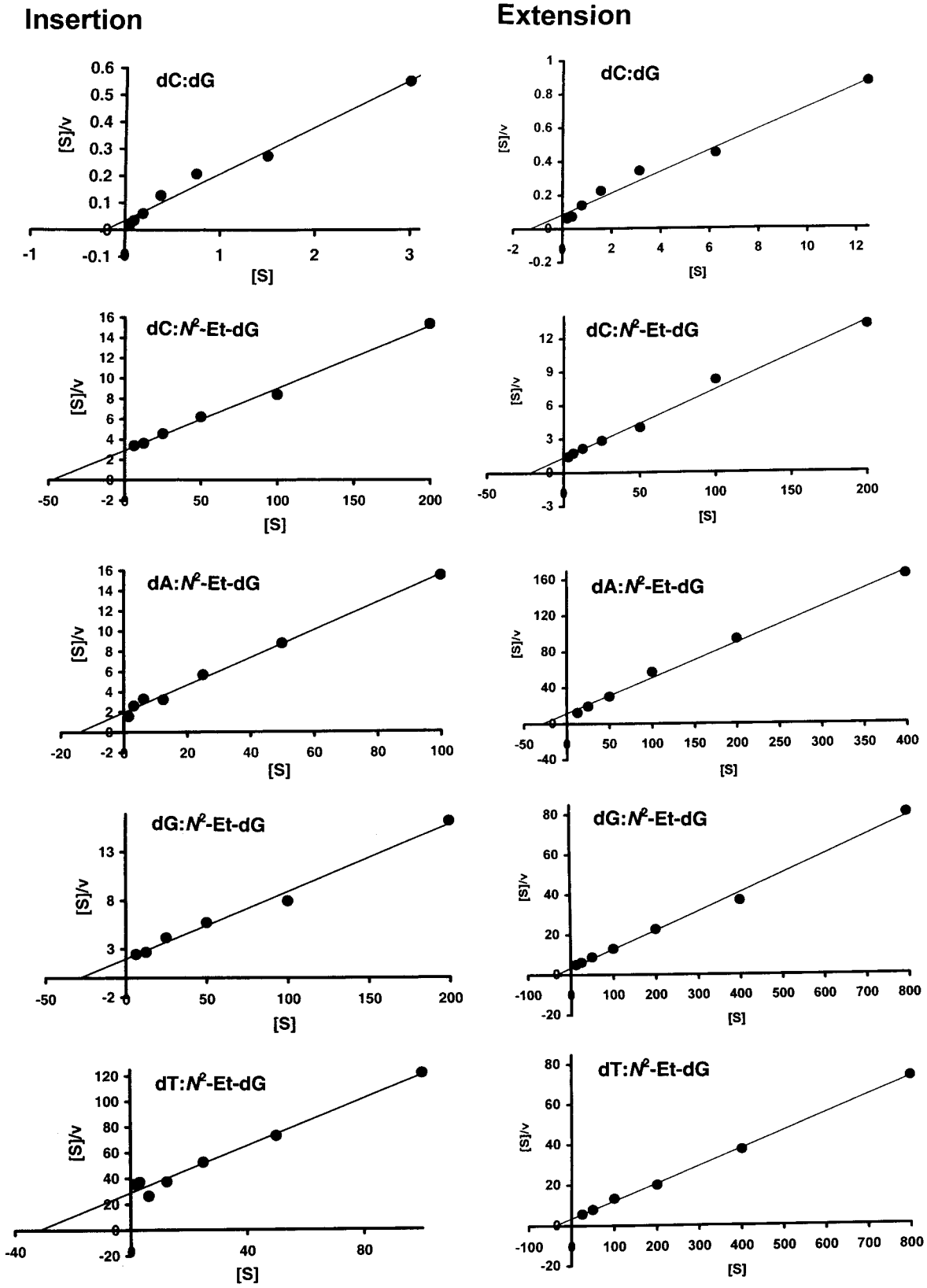

FIGURE 7: Hanes−Woolf plots of deoxynucleotide insertion opposite the N^2-Et-dG lesion and chain extension. Using 1.0 pmol of 24-mer (5′CCTTCXCTTCTTTCCTCTCCCTTT, where X is dG or N^2-Et-dG) primed with 0.5 pmol of a ^{32}P-labeled 12-mer (5′AGAGGAAAGAAG), a reaction mixture containing 0.001−0.5 unit of the exo$^-$ KF and varying amounts of a single dNTP was incubated at 25 °C for 2 min in 10 μL of Tris-HCl buffer (pH 8.0) to determine nucleotide insertion kinetics. Reaction mixtures containing 1.0 pmol of 24-mer template primed with 0.5 pmol of ^{32}P-labeled 13-mer (5′AGAGGAAAGAAGN, where N is C, A, G, or T) and varying amounts of dGTP were used to determine the chain extension kinetics. The reaction mixture was subjected to 20% denaturating PAGE. K_m and V_{max} were obtained from Hanes−Woolf plots, as described in Materials and Methods.

Table 2: Kinetic Parameters for the N^2-Et-dGTP Insertion Reaction Catalyzed by the Exo$^-$ Klenow Fragment[a]

insertion			
dXTP ↓GAAGAAAGGAGA^{32P} $^{5'}$CCTTCNCTTC TTT CCTCTCCCTTT			
X·N	K_m (μM)	V_{max} (% min^{-1})	F_{ins}
G·C	5.62 ± 1.44	10400 ± 320	1.0
N^2-Et-dG·C	8.91 ± 2.82	1960 ± 750	1.20×10^{-1}
N^2-Et-dG·A	5.89 ± 3.19	0.752 ± 0.016	6.96×10^{-5}
N^2-Et-dG·G	7.68 ± 1.70	2.22 ± 0.19	1.57×10^{-4}
N^2-Et-dG·T	19.3 ± 0.40	1.46 ± 0.50	4.11×10^{-5}

[a] The kinetics of dGTP or N^2-Et-dGTP insertion reactions were determined as described in Materials and Methods. Frequencies of nucleotide insertion (F_{ins}) were estimated with the equation $F = (V_{max}/K_m)_{[wrong\ pair]}/(V_{max}/K_m)_{[correct\ pair]}$, where X is dC, dA, dG, or dT. Data are expressed as means ± the standard deviation.

bands remained at position 13. The upper and lower bands represented the incorporation of dGMP and dCMP, respectively, opposite the N^2-Et-dG lesion. Since F_{ext} from the dC·N^2-Et-dG pair was 920 times higher than that for the dG·N^2-Et-dG pair, when incubated for a longer time (data not shown) or with large amounts of the exo$^-$ KF (Figure 5), the lower band representing the incorporation of dCMP opposite the N^2-Et-dG lesion disappeared faster than the upper band representing the incorporation of dGMP opposite the lesion. To explore how N^2-Et-dG can be paired with dC and dG, three-dimensional structures of the dC·N^2-Et-dG and dG·N^2-Et-dG pairs should be determined by NMR study or crystallography.

During DNA synthesis catalyzed by the exo$^-$ KF, significant amounts of one-base (9.7%) and two-base (7.1%) deletions also were detected. Since dGMP and dAMP were inserted opposite the N^2-Et-dG lesion, the newly inserted dGMP could be paired with dC 5′ to the lesion to form one-base deletions (Figure 6A) and the newly inserted dAMP could be paired with dT 5′ to the lesion to form two-base deletions (Figure 6B). These results follow from our proposed deletion mechanism originally described for the dG-C8-AAF DNA adduct (*26*).

The miscoding specificities of methylated DNA adducts such as 8-methyl-2′-deoxyguanosine (8-MedG) (*27*), O^6-methyl-2′-deoxyguanosine (O^6MedG) (*17*), and N^2-methyl-2′-deoxyguanosine (N^2-Me-dG) (*28*) have been determined by the same in vitro experimental system in our laboratory and compared to that of N^2-Et-dG. As summarized in Table 3, 8-MedG represents weak miscoding potential (*27*). In contrast, O^6MedG is a strong miscoding lesion, generating primarily G → A transitions (*17*). N^2-Me-dG promotes preferential incorporation of the correct base, dCMP, as similarly observed for 8-MedG, and also promoted a significant amount of incorporation of dTMP opposite the lesion, generating G → A transitions (*28*). The position of methylation on dG adducts significantly influences the miscoding specificity and frequency. The ethyl moiety of N^2-Et-dG and the methyl moiety of N^2-Me-dG are at the same position. Therefore, N^2-Et-dG could be expected to promote a miscoding specificity similar to that of N^2-Me-dG. However, N^2-Et-dG is a strong miscoding lesion, generating G → C mutations. This miscoding spectrum is different from that observed with N^2-Me-dG, where there were no G → C mutations (*28*). This indicates that the nature of the N^2 moiety also affects the miscoding specificity and frequency.

Table 3: Base Incorporation on Methyl- and Ethyl-Modified DNA Templates in Reactions Catalyzed by the Exo$^-$ Klenow Fragment

DNA adduct	C[e] (%)	A (%)	G (%)	T (%)	Δ^1 (%)	Δ^2 (%)	total miscoding frequency (%)
8-MedG[a]	77.0	0.41	1.10	nd[f]	0.38	0.81	2.7
O^6MedG[b]	5.27	nd	nd	75.5	nd	nd	75.5
N^2-Me-dG[c]	84.0	nd	nd	9.4	nd	nd	9.4
N^2-Et-dG[d]	39.0	2.2	40.0	1.9	9.7	7.1	60.9

[a] Data were taken from Kohda et al. (*27*). [b] Data were taken from Shibutani (*17*). [c] Data were taken from Yasui et al. (*28*). [d] Data were taken from Figure 6. [e] Expressed as the fraction of starting primer converted to the fully extended product. [f] nd, not detectable.

N^2-Et-dGTP was preferentially incorporated opposite template dC during DNA synthesis catalyzed by the exo$^-$ KF. F_{ins} of N^2-Et-dGTP opposite template dC was 760 times higher than that of N^2-Et-dGTP opposite template dG and only 8.3 times lower than that of dGTP opposite template dC (Table 1). F_{ins} of dCTP (7.92×10^{-4}) opposite the N^2-Et-dG lesion in DNA was 44 times lower than that reported for 7,8-dihydro-8-deoxyguanosine (8-oxodG) (1.18×10^{-2}) with the exo$^-$ KF (*29*). However, F_{ins} of N^2-Et-dGTP (1.20×10^{-1}) opposite template dC was 18 500 times higher than that for 8-oxodGTP (6.47×10^{-6}) (*30*). The level of utilization of N^2-Et-dGTP during DNA synthesis was much higher than that for 8-oxo-dGTP, as similarly observed with pol α and pol δ (*16*). Thus, N^2-Et-dG lesions formed by efficient incorporation of N^2-Et-dGTP into DNA may also cause mutations, generating G → C transversions in living cells.

The N^2-Et-dG DNA adduct has been detected in liver of mice treated with ethanol (*14*) and in white blood cells of alcohol abusers (*15*). Detection of N^2-Et-dG in the urine of nonalcohol drinkers indicates that humans are exposed to acetaldehyde without ingesting alcoholic beverages (*16*). Therefore, if N^2-Et-dG DNA adducts are not repaired, miscoding occurs at the lesion during translesional synthesis and may lead to the development of alcohol- or acetaldehyde-induced cancers.

REFERENCES

1. International Agency for Research on Cancer (1985) *IARC monographs on the Evaluation of Carcinogenic Risk of Chemicals to Humans: Allyl Compounds, Aldehydes, Epoxides and Peroxides*, Lyon, France.
2. International Agency for Research on Cancer (1985) *IARC monographs on the Evaluation of Carcinogenic Risk of Chemicals to Humans: Tobacco Smoking*, Lyon, France.
3. Jacobsen, E. (1950) *Biochim. Biophys. Acta 4*, 330−334.
4. Eriksson, C. J. P. (1980) *Les Colloques de l'INSERM, Alcohol and the Gastrointestinal Tract*, Vol. 95, pp 111−130, INSERM, Paris.
5. Franceshi, S., Taramini, R., Barra, S., et al. (1990) *Cancer Res. 50*, 6502−6507.
6. Hori, H., Kawano, T., Endo, M., and Yuasa, Y. (1997) *J. Clin. Gastroenterol. 25*, 568−575.
7. Obe, G., Natarajan, A. T., Meyers, M., and Hertog, A. D. (1979) *Mutat. Res. 68*, 291−294.
8. Korte, A., and Obe, G. (1981) *Mutat. Res. 88*, 389−395.
9. He, S. M., and Lambert, B. (1985) *Mutat. Res. 158*, 201−208.

10. Bariliak, I. R., and Kozachuk, S. Y. (1983) *Tsitol. Genet. 17*, 57−60.
11. Grafstrom, R. C., Dypbukt, J. M., Sundqvist, K., Atzori, L., Nielsen, I., Curren, R. D., and Harris, C. C. (1994) *Carcinogenesis 15*, 985−990.
12. Matsuda, T., Kawanishi, M., Yagi, T., Matsui, S., and Takebe, H. (1998) *Nucleic Acids Res. 26*, 1769−1774.
13. International Agency for Research on Cancer (1999) *IARC monographs on the Evaluation of Carcinogenic Risk of Chemicals to Humans: Re-evaluation of some organic chemicals, hydrazine and hydrogen peroxide (part two)*, Lyon, France.
14. Vaca, C. E., Fang, J. L., and Schweda, E. K. H. (1995) *Chem.-Biol. Interact. 98*, 51−67.
15. Fang, J. L., and Vaca, C. E. (1997) *Carcinogenesis 18*, 627−632.
16. Matsuda, T., Terashima, I., Matsumoto, Y., Yabushita, H., Matsui, S., and Shibutani, S. (1999) *Biochemistry 38*, 929−935.
17. Shibutani, S. (1993) *Chem. Res. Toxicol. 6*, 625−629.
18. Shibutani, S., Suzuki, N., Matsumoto, Y., and Grollman, A. P. (1996) *Biochemistry 35*, 14992−14998.
19. Boryski, J., and Ueda, T. (1985) *Nucleosides Nucleotides 4*, 595−606.
20. Takeshita, M., Chang, C.-N., Johnson, F., Will, S., and Grollman, A. P. (1987) *J. Biol. Chem. 262*, 10171−10179.
21. Shibutani, S., Bodepudi, V., Johnson, F., and Grollman, A. P. (1993) *Biochemistry 32*, 4615−4621.
22. Mendelman, L. V., Boosalis, M. S., Petruska, J., and Goodman, M. F. (1989*) J. Biol. Chem. 264*, 14415−14423.
23. Mendelman, L. V., Petruska, J., and Goodman, M. F. (1990) *J. Biol. Chem. 265*, 2338−2346.
24. Beaucage, S. L. (1993) in *Method in Molecular Biology, Protocols for oligonucleotides and analogues* (Agrawal, S., Ed.) Vol. 20, pp 33−61, Humana Press Inc., Totowa, NJ.
25. Terashima, I., Suzuki, N., Dasaradhi, L., Tan, C.-K., Downey, K. M., and Shibutani, S. (1998) *Biochemistry 37*, 13807−13815.
26. Shibutani, S., and Grollman, A. P. (1993) *J. Biol. Chem. 268*, 11703−11710.
27. Kohda, K., Tsunomoto, H., Minoura, Y., Tanabe, K., and Shibutani, S. (1996) *Chem. Res. Toxicol. 9*, 1278−1284.
28. Yasui, M., Matsui, M., Ihara, M., Santosh Laxmi, Y. R., Shibutani, S., and Matsuda, T. (2001) *Nucleic Acids Res.* (in press).
29. Lowe, L. G., and Guengerich, F. P. (1996) *Biochemistry 35*, 9840−9849.
30. Einolf, H. J., Schnetz-Boutaud, N., and Guengerich, F. P. (1998) *Biochemistry 37*, 13300−13312.

BI002719P